Report

Current Biology

The Aurora-A/TPX2 Axis Directs Spindle Orientation in Adherent Human Cells by Regulating NuMA and Microtubule Stability

Graphical Abstract

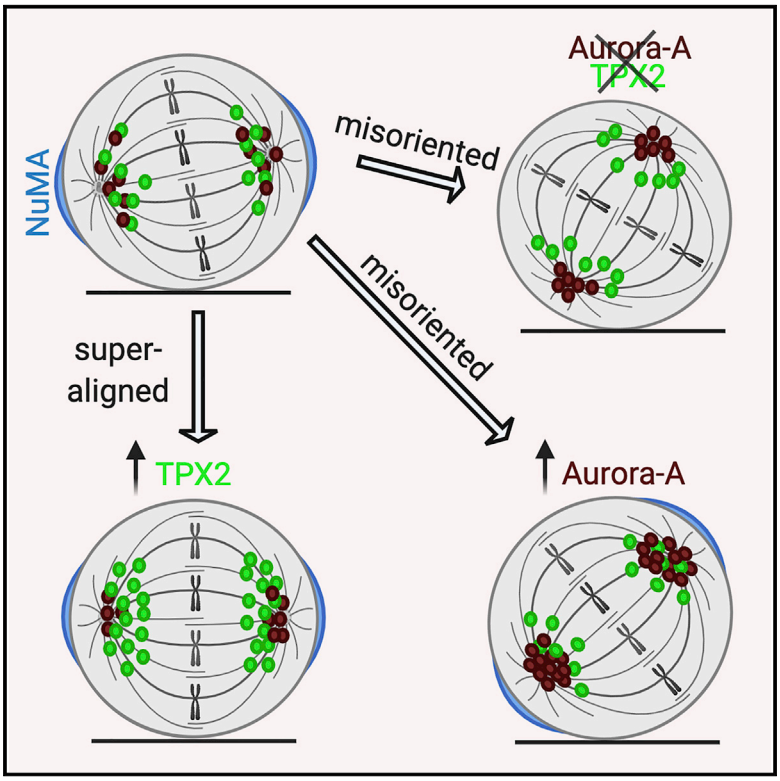

Highlights

- TPX2 is required for Aurora-A-mediated regulation of NuMA localization
- TPX2 and NuMA belong to the same complex at mitotic spindle poles
- TPX2 overexpression yields Aurora-A-independent metaphase spindle super-alignment
- Aurora-A increased levels yield spindle misorientation independently of NuMA

Authors

Federica Polverino, Francesco D. Naso, Italia A. Asteriti, ..., Alessandro Rosa, Marina Mapelli, Giulia Guarguaglini

Correspondence

marina.mapelli@ieo.it (M.M.), giulia.guarguaglini@uniroma1.it (G.G.)

In Brief

Polverino et al. investigate the role of the Aurora-A/TPX2 axis in spindle orientation in mammalian cells. They reveal a key role of TPX2 in Aurora-A-mediated control of NuMA localization. They also describe opposite and microtubule-dependent effects of increasing Aurora-A or TPX2 levels yielding misoriented or super-aligned spindles, respectively.

Polverino et al., 2021, Current Biology *31*, 1–10
February 8, 2021
https://doi.org/10.1016/j.cub.2020.10.096

CellPress

Current Biology

CellPress

Report

The Aurora-A/TPX2 Axis Directs Spindle Orientation in Adherent Human Cells by Regulating NuMA and Microtubule Stability

Federica Polverino,[1,2] Francesco D. Naso,[1] Italia A. Asteriti,[1] Valentina Palmerini,[2] Divya Singh,[3] Davide Valente,[1] Alexander W. Bird,[3] Alessandro Rosa,[4,5] Marina Mapelli,[2,6,*] and Giulia Guarguaglini[1,6,7,*]

[1]Institute of Molecular Biology and Pathology, National Research Council of Italy, c/o Department of Biology and Biotechnology, Sapienza University of Rome, Via degli Apuli 4, 00185 Rome, Italy

[2]Department of Experimental Oncology, IEO European Institute of Oncology IRCCS, Via Adamello 16, 20141 Milan, Italy

[3]Max Planck Institute of Molecular Physiology, Otto-Hahn-Str. 11, 44227 Dortmund, Germany

[4]Center for Life Nano Science, Istituto Italiano di Tecnologia, Viale Regina Elena 291, 00161 Rome, Italy

[5]Department of Biology and Biotechnology "C. Darwin," Sapienza University of Rome, Piazzale Aldo Moro 5, 00185 Rome, Italy

[6]These authors contributed equally

[7]Lead Contact

*Correspondence: marina.mapelli@ieo.it (M.M.), giulia.guarguaglini@uniroma1.it (G.G.)

https://doi.org/10.1016/j.cub.2020.10.096

SUMMARY

Mitotic spindle orientation is a crucial process that defines the axis of cell division, contributing to daughter cell positioning and fate, and hence to tissue morphogenesis and homeostasis.[1,2] The trimeric NuMA/LGN/Gαi complex, the major determinant of spindle orientation, exerts pulling forces on the spindle poles by anchoring astral microtubules (MTs) and dynein motors to the cell cortex.[3,4] Mitotic kinases contribute to correct spindle orientation by regulating nuclear mitotic apparatus protein (NuMA) localization,[5–7] among which the Aurora-A centrosomal kinase regulates NuMA targeting to the cell cortex in metaphase.[8,9] Aurora-A and its activator targeting protein for Xklp2 (TPX2) are frequently overexpressed in cancer,[10–12] raising the question as to whether spindle orientation is among the processes downstream the Aurora-A/TPX2 signaling axis altered under pathological conditions. Here, we investigated the role of TPX2 in the Aurora-A- and NuMA-dependent spindle orientation. We show that, in cultured adherent human cells, the interaction with TPX2 is required for Aurora-A to exert this function. We also show that Aurora-A, TPX2, and NuMA are part of a complex at spindle MTs, where TPX2 acts as a platform for Aurora-A regulation of NuMA. Interestingly, excess TPX2 does not influence NuMA localization but induces a "super-alignment" of the spindle axis with respect to the substrate, although an excess of Aurora-A induces spindle misorientation. These opposite effects are both linked to altered MT stability. Overall, our results highlight the importance of TPX2 for spindle orientation and suggest that spindle orientation is differentially sensitive to unbalanced levels of Aurora-A, TPX2, or the Aurora-A/TPX2 complex.

RESULTS AND DISCUSSION

The Aurora-A/TPX2 Complex Is Required for NuMA Localization and Spindle Orientation in Cultured Human Cells

In order to investigate whether the role of Aurora-A in spindle orientation requires TPX2-mediated activation, we used clonal U2OS cell lines stably expressing GFP-tagged mouse TPX2 (mTPX2), either wild type (WT) or deleted of the first 33 amino acids (hereon mTPX2$^{\Delta N}$) required for the direct interaction between TPX2 and the catalytic domain of Aurora-A.[13,14] mTPX2$^{\Delta N}$ is thus unable to immunoprecipitate Aurora-A, in contrast to mTPX2^{WT}. The effects of impairing Aurora-A/TPX2 complex formation can therefore be assessed by comparing the two mTPX2-expressing cell lines (either WT or ΔN) after RNA interference (RNAi)-mediated depletion of endogenous TPX2.[14] This allows investigation of TPX2 function in metaphase (Figure S1A), as depletion of TPX2 alone causes a strong prometaphase arrest.[15,16] As expected, the Aurora-A/TPX2 interaction was abolished in hTPX2-interfered/mTPX2$^{\Delta N}$-expressing cells (Figure S1B), in which Aurora-A localization was restricted to centrosomes and absent from microtubules (MTs) (Figure S1A). The specificity of the Aurora-A mislocalization was confirmed by the unaltered distribution of the kinesin Eg5, a different TPX2 interactor (Figure S1C). Aurora-A auto-phosphorylation on Thr288 was strongly reduced in hTPX2-interfered/mTPX2$^{\Delta N}$-expressing mitoses (Figures S1D and S1E), suggesting that pThr288-dependent activation of Aurora-A requires binding to TPX2.

When measuring the orientation of metaphase spindle axes with respect to the substrate using the average deviations from

Please cite this article in press as: Polverino et al., The Aurora-A/TPX2 Axis Directs Spindle Orientation in Adherent Human Cells by Regulating NuMA and Microtubule Stability, Current Biology (2020), https://doi.org/10.1016/j.cub.2020.10.096

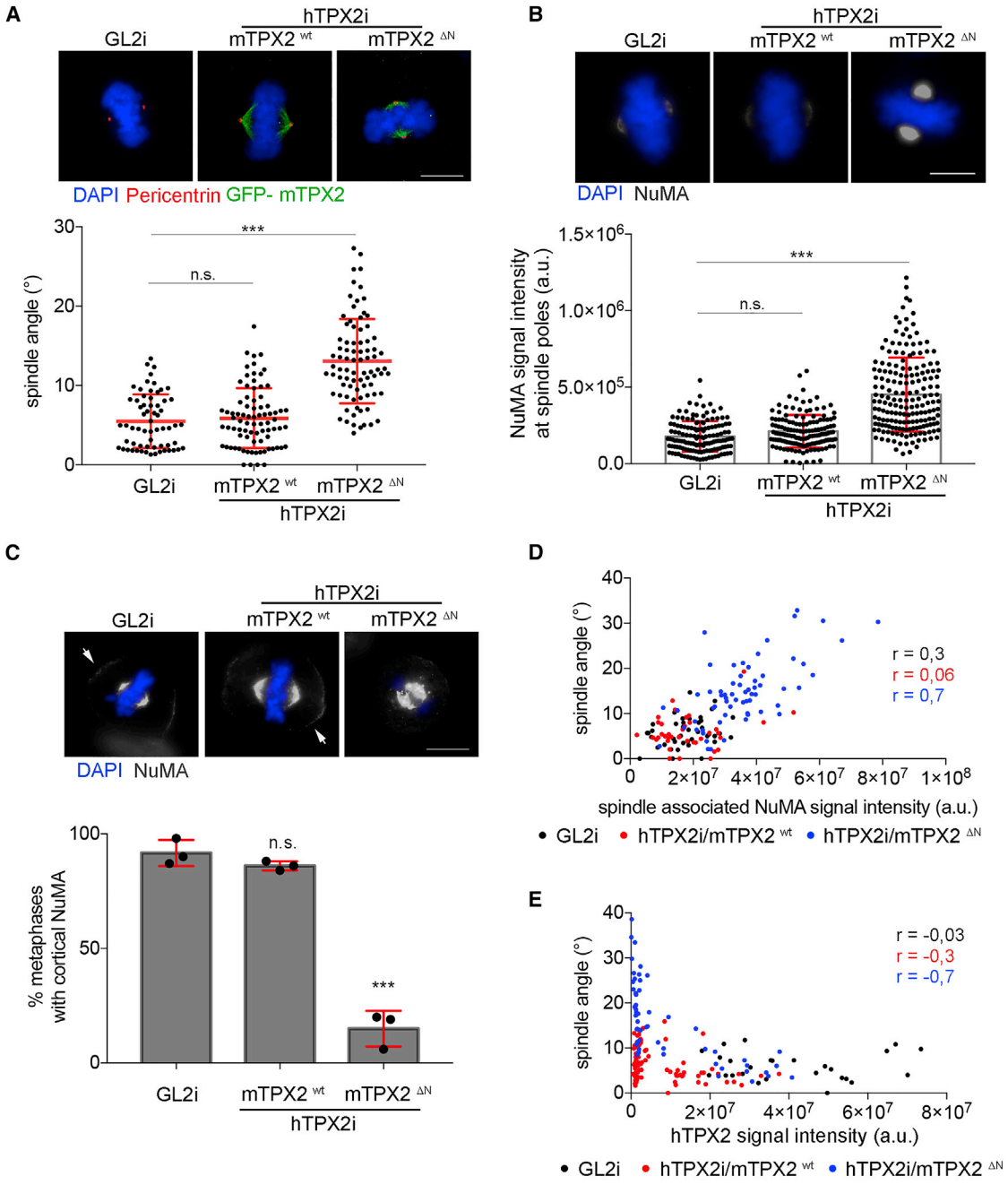

Figure 1. The Aurora-A/TPX2 Complex Controls Mitotic Spindle Orientation

(A–C) Distribution in the indicated cell lines of spindle angle values (A), NuMA signal intensity at each spindle pole (corrected for internal background; conservative fixation; B), and the percentage of metaphases displaying cortical NuMA (arrowed; pre-extraction and fixation; C). IF panels for each condition are shown. (D and E) NuMA (D) or TPX2 (E) signal intensity at metaphase spindles against the spindle angle values for each single cell, under the indicated conditions. The mouse anti-TPX2 antibody (Abcam) was used to quantify endogenous hTPX2 because it did not recognize exogenous GFP-tagged mouse TPX2 (Figure S1F). Sample size per condition: at least 60 (A and B) or 150 (C) metaphases from 3 independent experiments; between 25 and 85 metaphases (D and E) from triplicate experiments. a.u., arbitrary units. Error bars: SD; n.s., not significant; ***$p < 0.0001$; ANOVA (A and B) or chi-square (and Fisher's exact) test (C). r, correlation values (D and E). Scale bars, 10 μm. See also Figures S1 and S4.

the horizontal orientation (0°; see STAR Methods for details), we found comparable angle distributions in control-interfered (GL2i) and TPX2-interfered/mTPX2^{WT}-expressing (hTPX2i/mTPX2^{WT}) U2OS cultures (mean angle of 5.5° and 5.9°, respectively). Conversely, an increase of about 7.5° in the spindle axis angles was observed in cells expressing mTPX2$^{\Delta N}$ following TPX2 RNAi (hTPX2i/mTPX2$^{\Delta N}$), indicating the importance of the Aurora-A/TPX2 complex for spindle orientation (Figure 1A). The observed

Please cite this article in press as: Polverino et al., The Aurora-A/TPX2 Axis Directs Spindle Orientation in Adherent Human Cells by Regulating NuMA and Microtubule Stability, Current Biology (2020), https://doi.org/10.1016/j.cub.2020.10.096

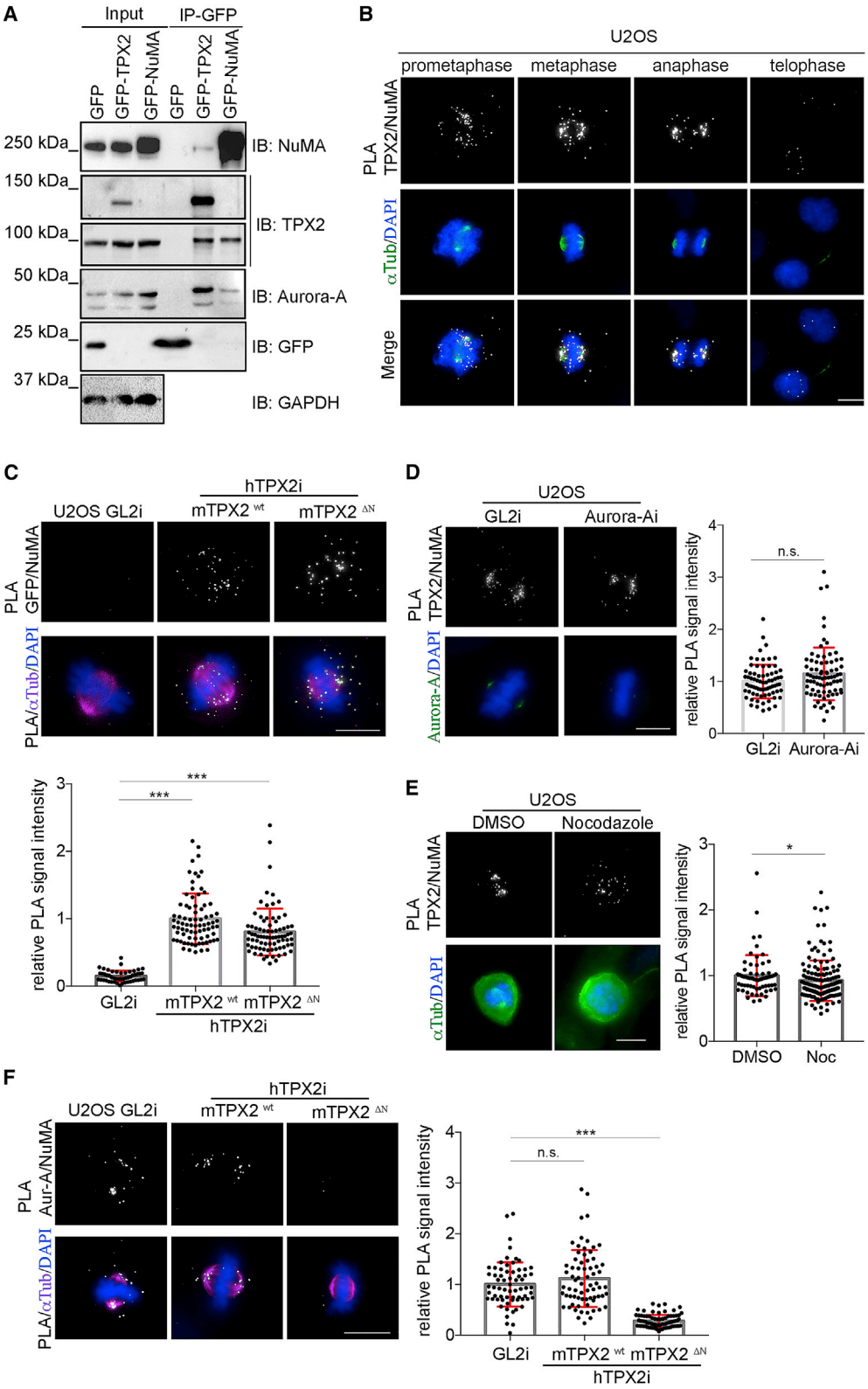

Figure 2. NuMA, TPX2, and Aurora-A Interact at Spindle Poles

(A) GFP-Trap immunoprecipitates from U2OS cells expressing exogenous GFP, GFP-TPX2, or GFP-NuMA analyzed by western blotting using the indicated antibodies. hTPX2 or exogenous GFP-mTPX2 are detected with the anti-TPX2 antibody (Novus Biologicals) on two regions (lower and upper panels, respectively) of the same membrane. Input total extracts (about 1/10 of the starting extract) for each IP are shown. GAPDH is a loading control.

(legend continued on next page)

Please cite this article in press as: Polverino et al., The Aurora-A/TPX2 Axis Directs Spindle Orientation in Adherent Human Cells by Regulating NuMA and Microtubule Stability, Current Biology (2020), https://doi.org/10.1016/j.cub.2020.10.096

defect was consistent with spindle misorientation observed following Aurora-A chemical inhibition by MLN8237,[8,17] which results in aberrant accumulation of the dynein-adaptor NuMA, due to a decreased mobility, at the spindle poles and its loss from the cortex.[8,9] To assess whether TPX2 is implicated in NuMA localization, NuMA was imaged by immunofluorescence (IF) in the mTPX2^{WT}- and mTPX2$^{\Delta N}$-expressing cell lines, using a conservative fixation to preserve the NuMA pool at spindle poles (Figure 1B) or a pre-extraction procedure prior to fixation to visualize cortical NuMA (Figure 1C). As expected, NuMA distribution at the cellular cortex and at the spindle poles in metaphase cells was comparable in GL2i cells and hTPX2i/mTPX2^{WT}-expressing cells. Importantly, in hTPX2i/mTPX2$^{\Delta N}$-expressing metaphases, NuMA was enriched at spindle poles (Figure 1B) and undetectable at the cell cortex (Figure 1C). Notably, single-cell analyses revealed that spindle misorientation correlates positively with increased levels of spindle-associated NuMA (Figure 1D) and negatively with residual levels of endogenous TPX2 in the cell lines (Figure 1E; see antibody characterization in Figure S1F). We conclude that, in U2OS cells, the TPX2-regulated pool of Aurora-A is involved in controlling NuMA distribution and spindle orientation. This result somehow differs from what is reported in HeLa cells,[9] where Aurora-A inhibition was able to counteract the enrichment of NuMA at the cell cortex induced by Cdk1 inhibition, while TPX2 partial depletion was not. Two not mutually exclusive explanations may account for this difference. First, under our experimental conditions, the TPX2-activated pool of Aurora-A may be more severely affected as compared to the reported TPX2 partial depletion.[9] Second, our conditions fully preserve TPX2 localization to spindle poles. It is thus possible that the Aurora-A-regulated fraction of NuMA that shuttles from the poles to the cortex requires the presence of TPX2 at the spindle poles not only to activate Aurora-A to phosphorylate NuMA but also to provide a scaffolding function to recruit NuMA to the poles.

TPX2 Interacts with NuMA at Spindle Poles and Favors Aurora-A/NuMA Interaction

To explore a putative scaffolding role of TPX2, we characterized the interaction between TPX2, Aurora-A, and NuMA by GFP immunoprecipitations (IPs) from GFP-TPX2 or GFP-NuMA transfected U2OS cells (Figures 2A and S2A). Interestingly, TPX2 and NuMA were found in the reciprocal IPs and Aurora-A was detected in both GFP-TPX2 and GFP-NuMA IPs. This indicates that the three proteins are part of the same macromolecular complex, either establishing direct contacts or requiring additional subunits, that likely favors NuMA phosphorylation by Aurora-A. We then used *in situ* proximity ligation assays (*is*PLA) to localize the NuMA/TPX2/Aurora-A interactions in mitotic cells and assess their interdependency. We detected NuMA/TPX2 *is*PLA signals at mitotic spindle poles from prometaphase until telophase (Figure 2B), after which TPX2 levels are physiologically downregulated.[18] NuMA/TPX2 *is*PLA signals were highly specific and were also detected in non-transformed hTERT-RPE-1 cells, supporting the biological relevance of the NuMA/TPX2 interaction (Figures S2B–S2D). *is*PLA reactions with the anti-GFP/anti-NuMA antibodies pair (Figure 2C) revealed that both GFP-tagged mTPX2^{WT} or mTPX2$^{\Delta N}$ are able to interact with NuMA, thus indicating that the interaction between TPX2 and NuMA occurs regardless of Aurora-A binding. TPX2/NuMA *is*PLA measurement in cells depleted of Aurora-A by RNAi confirmed that Aurora-A is not required for the interaction between endogenous TPX2 and NuMA (Figure 2D). Interestingly, MTs were also not required for the TPX2/NuMA interaction, as shown by *is*PLA assays performed in nocodazole-treated mitoses (Figure 2E). Intriguingly, the TPX2/NuMA interaction was detected in about one-third of interphases too (Figure S2E), where TPX2 and NuMA are compartmentalized within the nucleus.[15,19]

The evidence that TPX2 and NuMA are part of a protein complex supports the hypothesis that TPX2, beside activating Aurora-A, may have a scaffolding function in presenting NuMA to Aurora-A. If so, the regions of TPX2 involved in NuMA or Aurora-A binding should not overlap, as supported by the evidence that mTPX2$^{\Delta N}$ interacts with NuMA in *is*PLA assays (Figure 2C). Consistently, no competition between Aurora-A and NuMA for TPX2 binding emerged when measuring TPX2/NuMA interaction in cells where TPX2/Aurora-A interaction was increased by Aurora-A overexpression (Figure S2G). Notably, *is*PLA experiments showed that, in U2OS cells, the Aurora-A/NuMA interaction at spindles was not altered in hTPX2i/mTPX2^{WT}-expressing metaphases (Figure 2F, central column; controls in Figure S2F), while it was strongly reduced in hTPX2i/mTPX2$^{\Delta N}$-expressing ones (Figure 2F, right panels). Together, these results indicate that TPX2 contributes to NuMA localization and spindle orientation and suggest that it acts not only by activating Aurora-A but also by favoring the kinase-substrate interaction between Aurora-A and NuMA. We previously proposed the existence of a receptor for NuMA at spindle poles, whose affinity is reduced upon NuMA phosphorylation by Aurora-A to enable NuMA "poles-to-cortex" shuttling.[8] Our present results raise the intriguing possibility that the NuMA receptor at the spindle poles MTs is TPX2 itself. Interestingly, depletion or inactivating mutations of the PP6 phosphatase that specifically dephosphorylates Aurora-A within the Aurora-A/TPX2 complex[20] results in reduced levels of NuMA at spindle poles.[21]

Increased TPX2 Levels Induce a Spindle Superalignment Phenotype

When measuring spindle orientation in mTPX2^{WT}-expressing U2OS, we noticed that, in cultures where endogenous TPX2 was not RNAi depleted (GL2i/mTPX2^{WT}), which are expected to display a moderate increase of TPX2 levels (about 2-fold),[14]

(B–F) TPX2/NuMA *is*PLA signals at the spindle in U2OS cells are shown in different mitotic substages (B), in Aurora-A-interfered mitoses (D), or following nocodazole treatment (Noc) (E). GFP-mTPX2/NuMA (C) or Aurora-A/NuMA (F) *is*PLA signals under the indicated conditions are shown and quantified in the dot plots. Specific antibodies pairs used for each *is*PLA reaction are defined in the STAR Methods section and Key Resources Table. Values were normalized to the average control (GL2i or DMSO) in each experiment. Sample size for each condition is as follows: at least 50 prometa- (E) or metaphases (C, D, and F) from 3 independent experiments. Error bars: SD; n.s., not significant; *$p < 0.01$; ***$p < 0.0001$; ANOVA (C and F) or Mann-Whitney (D and E) test. Scale bars, 10 μm.
See also Figure S2.

Please cite this article in press as: Polverino et al., The Aurora-A/TPX2 Axis Directs Spindle Orientation in Adherent Human Cells by Regulating NuMA and Microtubule Stability, Current Biology (2020), https://doi.org/10.1016/j.cub.2020.10.096

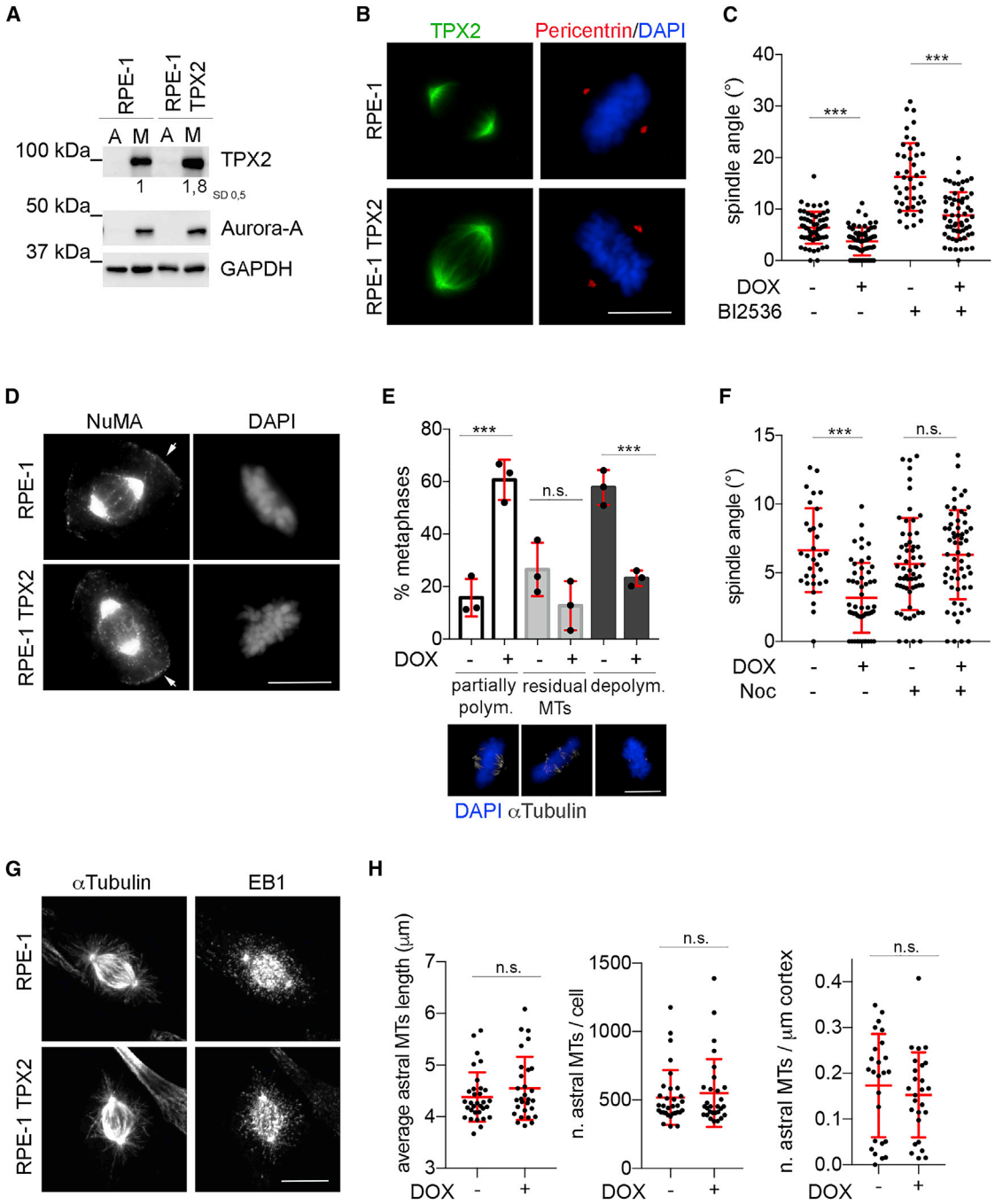

Figure 3. Spindle Orientation in TPX2-Overexpressing hTERT-RPE-1 Cell Lines

(A) Immunoblotting with TPX2 and Aurora-A antibodies in mitotic (M) and asynchronous (A) total lysates of TPX2-overexpressing cultures (24 h of doxycycline [DOX] induction; indicated as RPE-1 TPX2 throughout the figure) and non-induced controls (indicated as RPE-1 throughout the figure). GAPDH was a loading control. Average fold increase of TPX2 levels in mitotic extracts after induction is shown; subscripts indicate standard deviations, 3 independent experiments.

(B) IF panels show TPX2 (green) in control or DOX-induced metaphases.

(C) Dot plot of the spindle angle values in induction (DOX) and PLK1 inhibition (BI2536).

(D) NuMA localization in metaphases in the indicated conditions.

(E) Percentage of metaphases showing (1) partially polymerized, (2) few residual only, or (3) totally depolymerized spindle MTs after 15 min ice incubation under the indicated conditions (exemplifying α-tubulin images in IF panels below).

(F) Spindle angle values in control or DOX-induced metaphases following low Noc treatment are shown in the dot plots.

(G) IF panels show astral MTs length and abundance (α-tubulin and EB1 staining).

(legend continued on next page)

Please cite this article in press as: Polverino et al., The Aurora-A/TPX2 Axis Directs Spindle Orientation in Adherent Human Cells by Regulating NuMA and Microtubule Stability, Current Biology (2020), https://doi.org/10.1016/j.cub.2020.10.096

spindles were more aligned to the substrate compared to control cells (GL2i; Figure S2H). To further investigate the effects of TPX2 overexpression, a condition frequently observed in cancer cells,[10,22] on mitotic spindle orientation, we generated a cellular system for stable inducible FLAG-TPX2 overexpression in hTERT-RPE-1 non-transformed cellular background (Figures 3A and 3B). The TPX2 about 2-fold increase was comparable to that observed in the mTPX2^{WT}-expressing U2OS, avoiding prometaphase arrest observed at higher TPX2 levels.[15,23] Consistent with TPX2 roles in MT nucleation,[24–26] in the hTERT-RPE-1 line stably overexpressing TPX2, the spindle MT mass appeared significantly increased compared with control cells (Figure S3A). Interestingly, also these TPX2-overexpressing hTERT-RPE-1 cells display "super-aligned" spindles (Figure 3C), with TPX2 levels negatively correlating with spindle angle values in single-cell analyses (Figure S3B), indicating a correlation between the super-alignment phenotype and TPX2 overexpression. Given the small deviation in the average spindle axis angle in control RPE cells (about 6.4°), in order to assess the significance of the observed super-alignment phenotype, the spindle orientation was independently challenged in TPX2-overexpressing metaphases. To this aim, cultures were treated with a PLK1 inhibitor, a condition reported to affect spindle orientation through enrichment of cortical NuMA levels,[7] which revealed that TPX2-overexpressing cells are more resistant to spindle misorientation induced by PLK1 inhibition compared to control cells (Figure 3C; BI2536-treated samples). Importantly, no correlation between p-Thr288 Aurora-A levels and spindle orientation in TPX2-overexpressing metaphases was observed, suggesting that the super-alignment phenotype does not depend on increased Aurora-A activity (Figure S3C). In addition, consistent with the robust spindle alignment displayed in TPX2 overexpression conditions, NuMA correctly localizes at spindle poles and cell cortex, indicating that NuMA distribution is not sensitive to TPX2 increased levels (Figures 3D, S3D, and S3E).

We surmised that MT dynamic properties may be a cellular parameter affected in TPX2-overexpressing cells and relevant for spindle orientation. To verify spindle MTs stability, we first conducted MT depolymerization in the cold under our mild TPX2 overexpression conditions (Figure 3E). In control cultures (DOX−), after 15 min on ice, only about 15% metaphases displayed polymerized spindle MTs, while about 25% and 60% displayed few sparse MTs only or no MTs, respectively. Conversely, in TPX2-overexpressing cultures, about 60% metaphases still displayed partially polymerized MTs, and only 23% did not show MTs at all, indicating that TPX2 overexpression induces increased MT stability. We then analyzed spindle orientation after treatment of TPX2-overexpressing cells with low doses of nocodazole known to affect astral MTs and spindle orientation[27] without influencing spindle assembly and mitotic progression. Under these conditions, no defective spindle orientation *per se* was induced, and the spindle super-alignment induced by TPX2 overexpression was completely rescued (Figure 3F), suggesting that changes in astral MT function could be important for super-alignment. Although we did not observe any major changes in the length or number of growing EB1-labeled astral MTs or in the number of astral MTs reaching the cortex in the TPX2-overexpressing metaphases (Figures 3G and 3H), we cannot rule out that subtle changes in MT dynamics parameters in specific MT populations are present. It is also possible that TPX2 overexpression impacts on the TPX2 interaction with spindle-associated, actin-binding proteins, such as myosin 10[28] and adducin-1,[29] that stabilize the connection between astral MTs and the acto-myosin cortex, which is key for spindle-placement mechanisms.[3]

Aurora-A Overexpression Induces Spindle Misorientation by Altering MT Stability

Given the key role of TPX2 in Aurora-A regulation, it may be envisaged that excess of TPX2 yields effects overlapping with those induced by Aurora-A excess, with important implications in cancer as Aurora-A is also overexpressed in tumors and the complex is regarded as both oncogenic unit and potential therapeutic target.[10,30,31] To explore the effects of increased levels of Aurora-A on spindle orientation, we generated an independent hTERT-RPE-1 cell line for stable and inducible expression of MYC-tagged Aurora-A (Figure 4), yielding an about 2-fold increase in Aurora-A levels (Figures 4A and 4B). Spindle angle measurements revealed that Aurora-A overexpression induced an opposite effect compared with TPX2 overexpression, with an increase in the mean spindle angle to about 11.5° versus 5.3° of control cells (Figure 4C), which spindle angle values directly correlated to Aurora-A levels (Figure S3F). IF analyses showed that no significant changes in NuMA localization at the cortex and poles occur upon Aurora-A overexpression, indicating that NuMA is not implicated in spindle misorientation in these cells (Figures 4D, S3D, and S3E). We conclude that NuMA localization is highly sensitive to disruption of the Aurora-A/TPX2 complex (Figure 1), but not to imbalances of the single components (Figures S3D and S3E).

Rather, upon Aurora-A overexpression, we observed increased lengths (but not overall abundance) of astral MTs (Figures 4E–4I), due to an increased fraction of longer MTs (i.e., >9 μm), which may reach the cortex (Figure 4H). This is consistent with a report of Aurora-A overexpression leading to increased MT assembly rates and defective spindle positioning in HCT-116 cell prometaphases, rescued in metaphase, which may reflect cancer cells compensatory mechanisms.[32] Indeed, treatment with sub-nanomolar doses (0.25 nM) of Taxol, reported to affect the stability of astral MTs[33] and to suppress both increased MT assembly rates and spindle mispositioning induced by Aurora-A overexpression,[32] restored correct spindle orientation in Aurora-A-overexpressing non-transformed cells (Figure 4J).

Given the opposite effects of TPX2 or Aurora-A overexpression on spindle orientation and their frequent concomitant

(H) Dot plots represent average astral MTs length (left) and number (central) per cell under labeled conditions. The number of MTs contacting the cell cortex per micrometer of cortex in 2 dimensions is shown in the dot plot on the right.

Sample size per condition: 25–60 metaphases (C, F, and H) and at least 100 counted metaphases (E) from 3 independent experiments. Error bars: SD; n.s., not significant; ***$p < 0.0001$; one-way ANOVA (C and F), chi-square (and Fisher's exact) test (E), and t test or Mann-Whitney test (H). Scale bars, 10 μm. See also Figures S3 and S4.

Please cite this article in press as: Polverino et al., The Aurora-A/TPX2 Axis Directs Spindle Orientation in Adherent Human Cells by Regulating NuMA and Microtubule Stability, Current Biology (2020), https://doi.org/10.1016/j.cub.2020.10.096

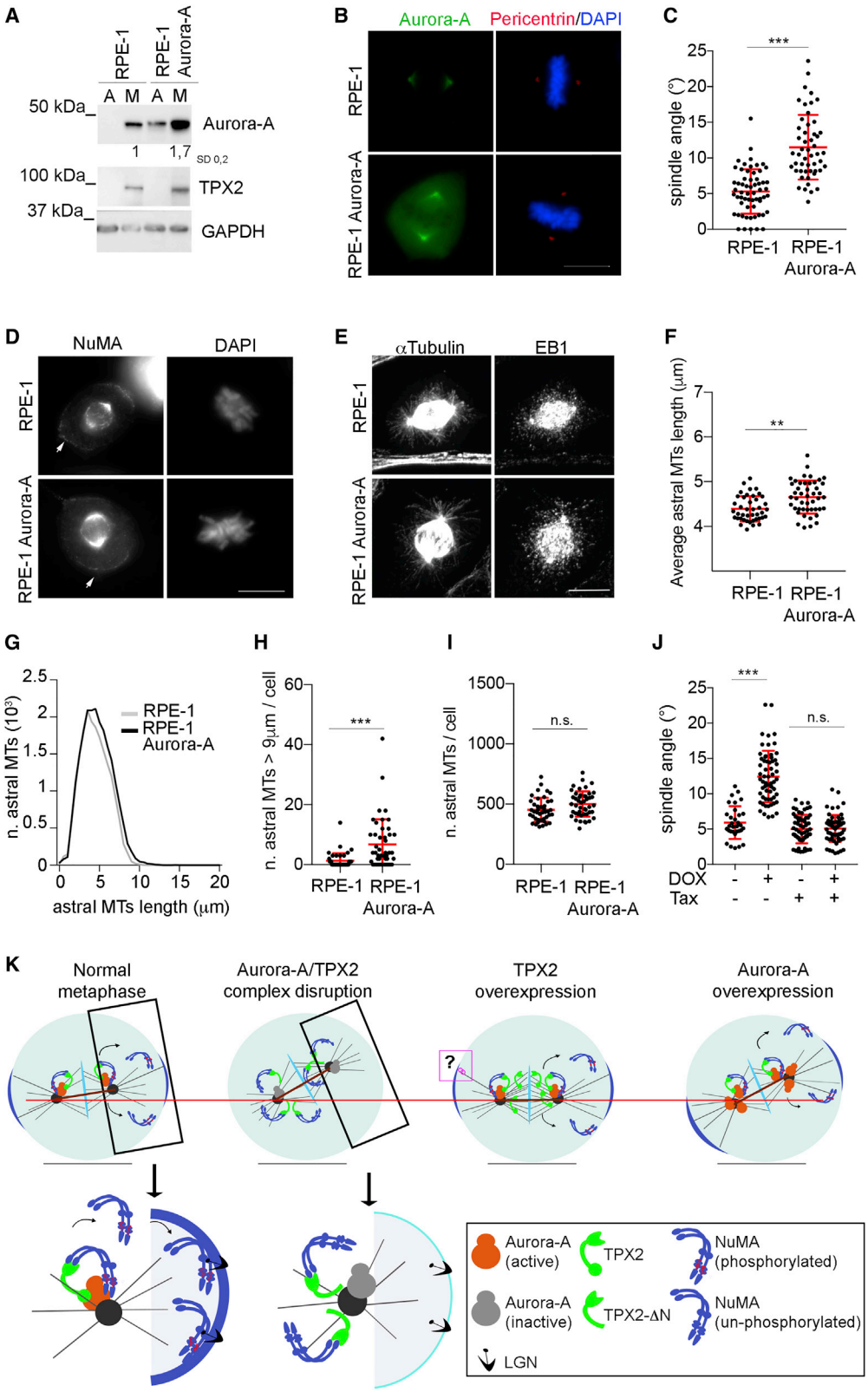

Figure 4. Spindle Orientation in Aurora-A-Overexpressing hTERT-RPE-1 Cell Lines

(A) Immunoblotting performed as described in Figure 3 on lysates of Aurora-A-overexpressing cultures (indicated as RPE-1 Aurora-A throughout the figure) with respect to non-induced controls (indicated as RPE-1 throughout the figure).

(legend continued on next page)

Please cite this article in press as: Polverino et al., The Aurora-A/TPX2 Axis Directs Spindle Orientation in Adherent Human Cells by Regulating NuMA and Microtubule Stability, Current Biology (2020), https://doi.org/10.1016/j.cub.2020.10.096

upregulation in cancer, we wondered what the consequences would be of co-overexpressing them. In the hTERT-RPE-1 system, Aurora-A/TPX2 stable co-overexpression led to a strong prometaphase enrichment associated with spindle and centrosome defects (our unpublished data), so that spindle orientation could not be evaluated. We thus introduced Aurora-A-mCherry in the mTPX2^{WT}-U2OS cell line used above (Figure S3G), which yielded mild overexpression of both proteins compatible with the presence of bipolar metaphase spindles. Under these conditions, the super-alignment phenotype observed with TPX2 overexpression alone was rescued; in addition, about 10% metaphases displayed a spindle axis angle >15°, which was never observed in control cultures (Figure S3G). Together, results indicate that Aurora-A overexpression causes spindle misorientation, thereby counterbalancing TPX2 overexpression-induced spindle super-alignment.

Overall, our findings indicate that the Aurora-A/TPX2 complex is necessary for spindle orientation in adherent mammalian cells in culture and for the first time reveal that Aurora-A, TPX2, and NuMA are part of a protein complex (Figure 4K). The TPX2/NuMA interaction is also evident in a fraction of interphase cells. Because for both proteins the nuclear localization signal overlaps with MT-binding regions,[25,34] existence of a nuclear TPX2/NuMA complex prior to mitotic entry could indicate a common regulation mode of the two proteins and may represent a regulatory step for the pool of NuMA undergoing Aurora-A phosphorylation at mitotic entry.

In addition, we demonstrate that overexpressing Aurora-A or TPX2 in non-transformed adherent hTERT-RPE-1 cells alters spindle orientation in opposite ways (Figure 4K). Aurora-A overexpression induces spindle misorientation; conversely, mild TPX2 overexpression yields a super-alignment phenotype. These effects appear largely independent of NuMA and involve MTs, whose chemical modulation restores normal spindle orientation in both situations. Because the orientation of cell division is crucial for tissue organization and homeostasis, it is tempting to speculate that these defects may represent one of the routes through which Aurora-A and TPX2 increased levels contribute to pathologies, e.g., by unbalancing the pool of proliferating/differentiating cells in stem cell niches. Interestingly, unbalances in Aurora-A or TPX2 levels were reported to alter the proportion of planar versus apicobasal divisions in muscle and neural stem cells and in the mammary epithelium, with implications in Duchenne muscular dystrophy, microcephaly, and cancer.[35–37] Relevance of anti-MT drugs and of inhibitors of Aurora-A, or recently of the Aurora-A/TPX2 interaction, in therapeutic approaches[12,31,38,39] further strengthen the importance of our results dissecting the multiple ways through which spindle orientation is driven by the Aurora-A/TPX2 axis.

STAR★METHODS

Detailed methods are provided in the online version of this paper and include the following:

- KEY RESOURCES TABLE
- RESOURCE AVAILABILITY
  - Lead Contact
  - Materials availability
  - Data and code availability
- EXPERIMENTAL MODEL AND SUBJECT DETAILS
  - Human cell lines
- METHOD DETAILS
  - Plasmids generation
  - Generation of stable cell lines
  - Synchronizations and treatments
  - siRNA oligonucleotides and plasmids transfection
  - Immunofluorescence (IF)
  - *in situ* Proximity Ligation Assays (*is*PLA)
  - Microscopy analyses on fixed samples
  - Spindle orientation analysis
  - Quantitative analysis of fluorescent signals
  - Immunoprecipitation (IP) assays and western blotting
- QUANTIFICATION AND STATISTICAL ANALYSIS

SUPPLEMENTAL INFORMATION

Supplemental Information can be found online at https://doi.org/10.1016/j.cub.2020.10.096.

ACKNOWLEDGMENTS

We thank Dalila Boi for experimental support. Microscopy experiments were performed at the IBPM Nikon Reference Centre. This work was supported by the Italian Association for Cancer Research (AIRC IG-17390 to G.G. and IG-18629 to M.M.), the Italian Ministry of Health (RF-2013-02357254 to M.M.), the Royal Society (International Exchange grant IES/RE/170195), and Regione Lazio (L.R. 13/08 project no. 85-2017-15348). This work was also partially supported by the Italian Ministry of Health with Ricerca Corrente

(B and C) IF panels (B) of Aurora-A (green) in control or DOX-induced metaphases, with spindle angle values reported in the dot plot in (C).
(D) NuMA localization in metaphases in the indicated conditions.
(E) IF panels show astral MT length and abundance (α-tubulin and EB1 staining) under labeled conditions.
(F, G, and I) Average astral MTs length (F), their normal distribution based on length (G), and abundance (I) per cell are represented.
(H) The number (per cell) of astral MTs with length >9 μm is represented.
(J) Spindle angle values in control or DOX-induced metaphases following low Taxol (Tax) treatment are shown in the dot plots. 30–60 measured metaphases per condition, from 3 independent experiments, are shown. Error bars: SD; n.s., not significant; **p < 0.001; ***p < 0.0001; t test or Mann-Whitney test (C, F, H, and I); one-way ANOVA (J). Scale bars, 10 μm.
(K) Schematic model of the role of the Aurora-A/TPX2 axis in spindle orientation control. In a normal metaphase, the Aurora-A/TPX2 complex interacts with and phosphorylates NuMA, allowing a pool of NuMA to reach the cortical region above the spindle poles. Aurora-A/TPX2 complex disruption (hTPX2i/mTPX2$^{\Delta N}$) results in the loss of the interaction between Aurora-A and NuMA that instead remains associated to TPX2. Unphosphorylated NuMA accumulates at the spindle poles and is simultaneously lost from the cell cortex. Overexpression of TPX2 or Aurora-A yield super-aligned or misoriented spindles, respectively. The red dashed line passing through the left centrosome of each panel and the pole-to-pole brick red line are used to better visualize differences in spindle alignment under the distinct experimental conditions. The boxed fuchsia chain represents our hypothesis of a tight link between astral MTs and cortex in TPX2-overexpressing cells.
See also Figures S3 and S4.

and 5x1000 funds to IEO. F.P. was partially supported by the TornoSubito Programme (Regione Lazio D.D. no. 1253, project 17694-16092019).

AUTHOR CONTRIBUTIONS

Conceptualization, G.G., M.M., and F.P.; Methodology, F.D.N., A.R., and D.V.; Investigation, I.A.A., F.D.N., F.P., V.P., and D.S.; Writing, G.G., M.M., and A.W.B.; Funding Acquisition, G.G. and M.M.

DECLARATION OF INTERESTS

The authors declare no competing interests.

Received: April 24, 2020
Revised: September 16, 2020
Accepted: October 30, 2020
Published: December 3, 2020

REFERENCES

1. Kulukian, A., and Fuchs, E. (2013). Spindle orientation and epidermal morphogenesis. Philos. Trans. R. Soc. Lond. B Biol. Sci. *368*, 20130016.
2. Morin, X., and Bellaïche, Y. (2011). Mitotic spindle orientation in asymmetric and symmetric cell divisions during animal development. Dev. Cell *21*, 102–119.
3. di Pietro, F., Echard, A., and Morin, X. (2016). Regulation of mitotic spindle orientation: an integrated view. EMBO Rep. *17*, 1106–1130.
4. Kiyomitsu, T. (2019). The cortical force-generating machinery: how cortical spindle-pulling forces are generated. Curr. Opin. Cell Biol. *60*, 1–8.
5. Kotak, S., and Gönczy, P. (2013). Mechanisms of spindle positioning: cortical force generators in the limelight. Curr. Opin. Cell Biol. *25*, 741–748.
6. Seldin, L., Poulson, N.D., Foote, H.P., and Lechler, T. (2013). NuMA localization, stability, and function in spindle orientation involve 4.1 and Cdk1 interactions. Mol. Biol. Cell *24*, 3651–3662.
7. Sana, S., Keshri, R., Rajeevan, A., Kapoor, S., and Kotak, S. (2018). Plk1 regulates spindle orientation by phosphorylating NuMA in human cells. Life Sci. Alliance *1*, e201800223.
8. Gallini, S., Carminati, M., De Mattia, F., Pirovano, L., Martini, E., Oldani, A., Asteriti, I.A., Guarguaglini, G., and Mapelli, M. (2016). NuMA phosphorylation by Aurora-A orchestrates spindle orientation. Curr. Biol. *26*, 458–469.
9. Kotak, S., Afshar, K., Busso, C., and Gönczy, P. (2016). Aurora A kinase regulates proper spindle positioning in C. elegans and in human cells. J. Cell Sci. *129*, 3015–3025.
10. Asteriti, I.A., Rensen, W.M., Lindon, C., Lavia, P., and Guarguaglini, G. (2010). The Aurora-A/TPX2 complex: a novel oncogenic holoenzyme? Biochim. Biophys. Acta *1806*, 230–239.
11. Joukov, V., and De Nicolo, A. (2018). Aurora-PLK1 cascades as key signaling modules in the regulation of mitosis. Sci. Signal. *11*, eaar4195.
12. Orth, M., Unger, K., Schoetz, U., Belka, C., and Lauber, K. (2018). Taxane-mediated radiosensitization derives from chromosomal missegregation on tripolar mitotic spindles orchestrated by AURKA and TPX2. Oncogene *37*, 52–62.
13. Bayliss, R., Sardon, T., Vernos, I., and Conti, E. (2003). Structural basis of Aurora-A activation by TPX2 at the mitotic spindle. Mol. Cell *12*, 851–862.
14. Bird, A.W., and Hyman, A.A. (2008). Building a spindle of the correct length in human cells requires the interaction between TPX2 and Aurora A. J. Cell Biol. *182*, 289–300.
15. Gruss, O.J., Wittmann, M., Yokoyama, H., Pepperkok, R., Kufer, T., Silljé, H., Karsenti, E., Mattaj, I.W., and Vernos, I. (2002). Chromosome-induced microtubule assembly mediated by TPX2 is required for spindle formation in HeLa cells. Nat. Cell Biol. *4*, 871–879.
16. De Luca, M., Lavia, P., and Guarguaglini, G. (2006). A functional interplay between Aurora-A, Plk1 and TPX2 at spindle poles: Plk1 controls centrosomal localization of Aurora-A and TPX2 spindle association. Cell Cycle *5*, 296–303.
17. Asteriti, I.A., Di Cesare, E., De Mattia, F., Hilsenstein, V., Neumann, B., Cundari, E., Lavia, P., and Guarguaglini, G. (2014). The Aurora-A inhibitor MLN8237 affects multiple mitotic processes and induces dose-dependent mitotic abnormalities and aneuploidy. Oncotarget *5*, 6229–6242.
18. Stewart, S., and Fang, G. (2005). Anaphase-promoting complex/cyclosome controls the stability of TPX2 during mitotic exit. Mol. Cell. Biol. *25*, 10516–10527.
19. Radulescu, A.E., and Cleveland, D.W. (2010). NuMA after 30 years: the matrix revisited. Trends Cell Biol. *20*, 214–222.
20. Zeng, K., Bastos, R.N., Barr, F.A., and Gruneberg, U. (2010). Protein phosphatase 6 regulates mitotic spindle formation by controlling the T-loop phosphorylation state of Aurora A bound to its activator TPX2. J. Cell Biol. *191*, 1315–1332.
21. Hammond, D., Zeng, K., Espert, A., Bastos, R.N., Baron, R.D., Gruneberg, U., and Barr, F.A. (2013). Melanoma-associated mutations in protein phosphatase 6 cause chromosome instability and DNA damage owing to dysregulated Aurora-A. J. Cell Sci. *126*, 3429–3440.
22. Pérez de Castro, I., and Malumbres, M. (2012). Mitotic stress and chromosomal instability in cancer: the case for TPX2. Genes Cancer *3*, 721–730.
23. Naso, F.D., Sterbini, V., Crecca, E., Asteriti, I.A., Russo, A.D., Giubettini, M., Cundari, E., Lindon, C., Rosa, A., and Guarguaglini, G. (2020). Excess TPX2 interferes with microtubule disassembly and nuclei reformation at mitotic exit. Cells *9*, 374.
24. Roostalu, J., Cade, N.I., and Surrey, T. (2015). Complementary activities of TPX2 and chTOG constitute an efficient importin-regulated microtubule nucleation module. Nat. Cell Biol. *17*, 1422–1434.
25. Zhang, R., Roostalu, J., Surrey, T., and Nogales, E. (2017). Structural insight into TPX2-stimulated microtubule assembly. eLife *6*, e30959.
26. Alfaro-Aco, R., Thawani, A., and Petry, S. (2017). Structural analysis of the role of TPX2 in branching microtubule nucleation. J. Cell Biol. *216*, 983–997.
27. Mora-Bermúdez, F., Matsuzaki, F., and Huttner, W.B. (2014). Specific polar subpopulations of astral microtubules control spindle orientation and symmetric neural stem cell division. eLife *3*, e02875.
28. Woolner, S., O'Brien, L.L., Wiese, C., and Bement, W.M. (2008). Myosin-10 and actin filaments are essential for mitotic spindle function. J. Cell Biol. *182*, 77–88.
29. Hsu, W.H., Wang, W.J., Lin, W.Y., Huang, Y.M., Lai, C.C., Liao, J.C., and Chen, H.C. (2018). Adducin-1 is essential for spindle pole integrity through its interaction with TPX2. EMBO Rep. *19*, e45607.
30. van Gijn, S.E., Wierenga, E., van den Tempel, N., Kok, Y.P., Heijink, A.M., Spierings, D.C.J., Foijer, F., van Vugt, M.A.T.M., and Fehrmann, R.S.N. (2019). TPX2/Aurora kinase A signaling as a potential therapeutic target in genomically unstable cancer cells. Oncogene *38*, 852–867.
31. Asteriti, I.A., Daidone, F., Colotti, G., Rinaldo, S., Lavia, P., Guarguaglini, G., and Paiardini, A. (2017). Identification of small molecule inhibitors of the Aurora-A/TPX2 complex. Oncotarget *8*, 32117–32133.
32. Ertych, N., Stolz, A., Stenzinger, A., Weichert, W., Kaulfuß, S., Burfeind, P., Aigner, A., Wordeman, L., and Bastians, H. (2014). Increased microtubule assembly rates influence chromosomal instability in colorectal cancer cells. Nat. Cell Biol. *16*, 779–791.
33. Gai, M., Bianchi, F.T., Vagnoni, C., Vernì, F., Bonaccorsi, S., Pasquero, S., Berto, G.E., Sgrò, F., Chiotto, A.M., Annaratone, L., et al. (2016). ASPM and CITK regulate spindle orientation by affecting the dynamics of astral microtubules. EMBO Rep. *17*, 1396–1409.
34. Chang, C.C., Huang, T.L., Shimamoto, Y., Tsai, S.Y., and Hsia, K.C. (2017). Regulation of mitotic spindle assembly factor NuMA by Importin-β. J. Cell Biol. *216*, 3453–3462.
35. Regan, J.L., Sourisseau, T., Soady, K., Kendrick, H., McCarthy, A., Tang, C., Brennan, K., Linardopoulos, S., White, D.E., and Smalley, M.J. (2013). Aurora A kinase regulates mammary epithelial cell fate by determining mitotic spindle orientation in a Notch-dependent manner. Cell Rep. *4*, 110–123.

36. Vargas-Hurtado, D., Brault, J.B., Piolot, T., Leconte, L., Da Silva, N., Pennetier, C., Baffet, A., Marthiens, V., and Basto, R. (2019). Differences in mitotic spindle architecture in mammalian neural stem cells influence mitotic accuracy during brain development. Curr. Biol. *29*, 2993–3005.e9.

37. Wang, Y.X., Feige, P., Brun, C.E., Hekmatnejad, B., Dumont, N.A., Renaud, J.M., Faulkes, S., Guindon, D.E., and Rudnicki, M.A. (2019). EGFR-Aurka signaling rescues polarity and regeneration defects in dystrophin-deficient muscle stem cells by increasing asymmetric divisions. Cell Stem Cell *24*, 419–432.e6.

38. Janeček, M., Rossmann, M., Sharma, P., Emery, A., Huggins, D.J., Stockwell, S.R., Stokes, J.E., Tan, Y.S., Almeida, E.G., Hardwick, B., et al. (2016). Allosteric modulation of AURKA kinase activity by a small-molecule inhibitor of its protein-protein interaction with TPX2. Sci. Rep. *6*, 28528.

39. Shi, J., and Mitchison, T.J. (2017). Cell death response to anti-mitotic drug treatment in cell culture, mouse tumor model and the clinic. Endocr. Relat. Cancer *24*, T83–T96.

40. Giubettini, M., Asteriti, I.A., Scrofani, J., De Luca, M., Lindon, C., Lavia, P., and Guarguaglini, G. (2011). Control of Aurora-A stability through interaction with TPX2. J. Cell Sci. *124*, 113–122.

41. Meraldi, P., Honda, R., and Nigg, E.A. (2002). Aurora-A overexpression reveals tetraploidization as a major route to centrosome amplification in p53-/- cells. EMBO J. *21*, 483–492.

42. Min, M., Mayor, U., and Lindon, C. (2013). Ubiquitination site preferences in anaphase promoting complex/cyclosome (APC/C) substrates. Open Biol. *3*, 130097.

43. Rosa, A., Papaioannou, M.D., Krzyspiak, J.E., and Brivanlou, A.H. (2014). miR-373 is regulated by TGFβ signaling and promotes mesendoderm differentiation in human Embryonic Stem Cells. Dev. Biol. *391*, 81–88.

44. Stout, J.R., Yount, A.L., Powers, J.A., Leblanc, C., Ems-McClung, S.C., and Walczak, C.E. (2011). Kif18B interacts with EB1 and controls astral microtubule length during mitosis. Mol. Biol. Cell *22*, 3070–3080.

45. Rondelet, A., Lin, Y.C., Singh, D., Porfetye, A.T., Thakur, H.C., Hecker, A., Brinkert, P., Schmidt, N., Bendre, S., Müller, F., et al. (2020). Clathrin's adaptor interaction sites are repurposed to stabilize microtubules during mitosis. J. Cell Biol. *219*, e201907083.

46. Singh, D., Schmidt, N., Müller, F., Bange, T., and Bird, A.W. (2020). Cdk1-dependent destabilization of long astral microtubules is required for spindle orientation. bioRxiv. https://doi.org/10.1101/2020.05.23.111989.

Please cite this article in press as: Polverino et al., The Aurora-A/TPX2 Axis Directs Spindle Orientation in Adherent Human Cells by Regulating NuMA and Microtubule Stability, Current Biology (2020), https://doi.org/10.1016/j.cub.2020.10.096

STAR★METHODS

KEY RESOURCES TABLE

REAGENT or RESOURCE	SOURCE	IDENTIFIER
Antibodies		
goat anti-actin	Santa Cruz Biotechnology	Cat#Sc1616 clonel-19; RRID: AB_630836
mouse anti-Aurora-A	BD Transduction Laboratories	Cat#610939; RRID: AB_398251
goat anti-Aurora-A	Abcam	Cat#Ab9689; RRID: AB_296564
rabbit anti-phospho-Aurora-A (Thr288)	Cell Signaling Technology	Cat#3079 clone C39D8; RRID: AB_2061481
rabbit anti-CEP-135	MPI CBG, Dresden	N.A.
mouse anti-mCherry	MPI CBG, Dresden	N.A.
rat anti-EB1	Absea Biotechnology	Cat#KT-51
rabbit anti-Eg5	Novus Biologicals	Cat#NB500-181; RRID: AB_10002881
mouse anti-GAPDH	Santa Cruz Biotechnology	Cat#Sc32233; RRID: AB_627679
mouse anti-GFP	Roche	Cat#11 814 460 001; RRID: AB_390913
rabbit anti-GFP	Abcam	Cat#Ab6556; RRID: AB_305564
mouse anti-NuMA	Millipore	Cat#MABE1807;
rabbit anti-NuMA	Abcam	Cat#Ab109262; RRID: AB_10863599
rabbit anti-pericentrin	Abcam	Cat#Ab4448; RRID: AB_304461
mouse anti-TPX2	Abcam	Cat#Ab32795; RRID: AB_778561
rabbit anti-TPX2	Novus Biologicals	Cat#NB500-179; RRID: AB_527246
rabbit anti-TPX2	Made in-house; MPI CBG, Dresden	[14]
chicken anti-α-tubulin	Abcam	Cat#Ab89984; RRID: AB_10672056
mouse anti-α-tubulin	Sigma-Aldrich	Cat#T5168; RRID: AB_477579
mouse anti-α-tubulin (DM1A)	Sigma-Aldrich	Cat#T6199; RRID: AB_477583
mouse anti-γ-tubulin	Sigma-Aldrich	Cat#T6557; RRID: AB_477584
Chemicals, Peptides, and Recombinant Proteins		
Lipofectamine LTX	Invitrogen	Cat#15338100
Oligofectamine	Invitrogen	Cat#12252011
Lipofectamine 2000	Invitrogen	Cat#11668019
Doxycycline hyclate	Santa Cruz Biotechnology	Cat#CAS 24390-14-5
Thymidine	Sigma-Aldrich	Cat#T1895
BI2536	Sigma-Aldrich	Cat#755038-02-9
Taxol	Sigma-Aldrich	Cat#T7402
Nocodazole	Sigma-Aldrich	Cat#M1404
Monastrol	Selleck Chemicals	Cat#S8439
poly-L-lysine	Sigma-Aldrich	Cat#P8920
Vectashield	Vector Laboratories	Cat#H-1000-10
Mowiol mounting medium	Calbiochem	Cat#4-88
Blasticidin-S hydrochloride	Sigma-Aldrich	Cat#15205
Puromycin	Sigma-Aldrich	Cat#P8833
Critical Commercial Assays		
in situ Proximity Ligation Assays	Sigma-Aldrich	Cat#DUO92007
GFP-Trap Magnetic Agarose	Chromotek	Cat#Gtma-20
Experimental Models: Cell Lines		
U2OS (epithelial osteosarcoma cells)	ATCC	HTB-96
U2OS expressing mouse GFP-TPX2 either wt or ΔN	[14]	N.A.

(*Continued on next page*)

Please cite this article in press as: Polverino et al., The Aurora-A/TPX2 Axis Directs Spindle Orientation in Adherent Human Cells by Regulating NuMA and Microtubule Stability, Current Biology (2020), https://doi.org/10.1016/j.cub.2020.10.096

Continued

REAGENT or RESOURCE	SOURCE	IDENTIFIER
U2OS expressing both mouse GFP-TPX2 and mCherry-Aurora-A	This manuscript	N.A.
hTERT-RPE-1 (cells of the retinal pigmented epithelium)	Kind gift of Prof. J. Pines	N.A.
hTERT-RPE-1 expressing either Aurora-A-MYC or FLAG-TPX2	This manuscript	N.A.
Oligonucleotides		
siRNA GL2: CGUACGCGGAAUACUUCGA	Ambion	[16]
siRNA Aurora-A: AUGCCCUGUCU UACUGUCA	Ambion	[16]
siRNA TPX2: GGGCAAAACUCCUUUGAGA	Ambion	[40]
MYC-TAA_UP 5′GATCCGAACAGAAACTGATTAGCGAA GAAGACCTGTA AGC-3′	This manuscript	N.A.
MYC-TAA_DN 5′GGCCGCTTACAGGTCTTCT TCGCTAATCAGTTTCTGTT CG-3′	This manuscript	N.A.
Recombinant DNA		
pEGFP-N1	Invitrogen	N/A
pEGFP-N1-hTPX2res	[40]	N/A
pEGFP- C1- Aurora-A	Kind gift of Prof. Dr. E.A. Nigg	[41]
pCDH-GFP-NuMA	[8]	N/A
epB-Puro-TT-FLAG-TPX2	[23]	N/A
epB-Bsd-TT-Aurora-A-MYC	This manuscript	N/A
Software and Algorithms		
Nis-Elements	Nikon	N/A
Photoshop CS 8.0.	Adobe	N/A
Image Lab 6.0.1	Biorad	N/A
Prism 7	Graphpad	N/A
Slidebook Software 6.0	Intelligent Imaging Innovations Inc.	N/A
Imaris 7.6.4	Bitplane	N/A
MATLAB R2018a	Mathworks	N/A

RESOURCE AVAILABILITY

Lead Contact

Further information and requests for resources and reagents should be directed to and will be fulfilled by the Lead Contact, Giulia Guarguaglini (giulia.guarguaglini@uniroma1.it).

Materials availability

Materials generated in this study can be obtained through the Lead Contact. There are restrictions to the availability of the constructs epB-Bsd-TT-Aurora-A-MYC and epB-Puro-TT-FLAG-TPX2 due to the fact that they are derivative of the ePiggyBac plasmid, provided by The Rockefeller University (New York, USA) to AR under an UMBTA.

Data and code availability

This study did not generate/analyze datasets/code.

EXPERIMENTAL MODEL AND SUBJECT DETAILS

Human cell lines

U2OS (female) and derived lines were grown in DMEM high glucose (Euroclone) supplemented with 10% FBS (Euroclone), penicillin-streptomycin (100 U/ml and 100 μg/ml; Sigma), 25 mM HEPES (Sigma), 4 mM L-glutamine (Euroclone). hTERT-RPE-1 (female) and derived lines were grown in DMEM/F12 (Dulbecco's Modified Eagle Medium F-12, Euroclone) supplemented with 10% tetracycline-free South American FBS (Aurogene) and other components as above. All cell lines were cultured at 37°C with 5% CO_2.

Please cite this article in press as: Polverino et al., The Aurora-A/TPX2 Axis Directs Spindle Orientation in Adherent Human Cells by Regulating NuMA and Microtubule Stability, Current Biology (2020), https://doi.org/10.1016/j.cub.2020.10.096

METHOD DETAILS

Plasmids generation

Plasmids for stable cell lines were generated as follows. The plasmid epB-Bsd-TT-Aurora-A-MYC was generated in two steps: (i) the sequence encoding for the fusion protein Aurora-A-Venus was excised from the pEYFP-N1_AuroraA plasmid[42] with the restriction enzymes BglII and NotI and cloned into the BamHI and NotI sites of the enhanced piggyBac transposable vector epB-Bsd-TT[43], (ii) then Venus sequence was excised by digestion with BamHI and NotI restriction enzymes and replaced with a sequence encoding for the MYC tag and including a stop codon, obtained by annealing the phosphorylated synthetic oligos MYC-TAA_UP and MYC-TAA_DN. The plasmid epB-Puro-TT-FLAG-TPX2 was generated as described in [23].

Generation of stable cell lines

Stable transgenic hTERT-RPE-1 cell lines expressing either Aurora-A-MYC or FLAG-TPX2 were generated by transfection of the epB-Bsd-TT-Aurora-A-MYC or epB-Puro-TT-FLAG-TPX2 plasmids, respectively, and the hyPB7 plasmid encoding the hyperactive piggyBac transposase. Transfections were performed using Lipofectamine LTX according to the manufacturer's instructions. Selection with blasticidin-S hydrochloride and puromycin (both 9 μg/ml) was applied after 48 h from transfection. Resistant cells were propagated as a pool and the expression of exogenous proteins was verified after administration of 1 μg/ml doxycycline.

The U2OS TPX2-LAP AuroraA-mCherry cell line was generated by stably transfecting the U2OS mTPX2(WT)-LAP cell clone[14] with a BAC containing AuroraA-mCherry with attached blasticidin resistance (MCB# 3197). This BAC was generated by recombineering of a C-terminal mCherry tag onto the C terminus of Aurora-A.

Synchronizations and treatments

For spindle orientation analyses hTERT-RPE-1 and derived cells were synchronized by 2 mM thymidine for 24 h and analyzed after 10-11 h from thymidine release; doxycycline (DOX) was added 24 h before fixation. When indicated, 30 minutes before fixation cultures were treated as follows: (i) BI2536 PLK1 inhibitor (300 nM;[7]), (ii) Taxol (0.25 nM;[33]), (iii) Nocodazole (30 pM,[27]). Single cell correlation analyses were performed on metaphase cells from asynchronous cultures. For MT depolymerization assays, cultures were incubated on ice for 15 min before fixation. For astral MT length analyses, asynchronous hTERT-RPE-1 and derived cells were treated with 1 μg/ml DOX for 24 h before fixing and staining.

siRNA oligonucleotides and plasmids transfection

Aurora-A, TPX2 and GL2 siRNA were used at the final concentration of 80 nM in asynchronously growing cultures, using Oligofectamine following the manufacturer's instructions. Note that the coding sequence for exogenous mTPX2 differs from that of endogenous hTPX2 in the region corresponding to the TPX2 siRNA oligonucleotides, so that mTPX2 results RNAi-resistant. Plasmids were used as follows: 4 μg (22 cm^2 dishes) for pEGFP-N1 or pEGFP-C1-Aurora-A; 10 μg (55 cm^2 dishes) of pEGFP-N1, pEGFP-N1-hTPX2res or pCDH-GFP-NuMA for GFP-Trap experiments. Transfections were performed in asynchronously growing U2OS cells, using Lipofectamine 2000 under the manufacturer's instructions.

Immunofluorescence (IF)

Cells plated on uncoated (hTERT-RPE-1) or poly-L-lysine-coted (U2OS) coverslips were fixed as follows: a) −20°C methanol, 6 min (pAurora-A and α-tubulin staining); b) PHEM (45 mM PIPES, 45 mM HEPES, 10 mM EGTA, 5 mM $MgCl_2$, pH 6.9) containing 0.3% Triton X-100, 4 min, followed by formaldehyde fixation as in (d) (NuMA at cell cortex); c) modified PHEM (30 mM PIPES, 12.5 mM HEPES, 5 mM EGTA, 2 mM $MgSO_4$) containing 0.25% Triton X-100 and 320 mM sucrose 15 s, followed by adding an equal volume of −20°C cold methanol for 45 s. Then, −20°C absolute methanol, 6 min (MT depolymerization assays); d) 3.7% formaldehyde plus 30 mM sucrose in PBS, 15 min (all other stainings), followed by permeabilization for 5 min at room temperature in PBS containing 0.1% Triton X-100. Blocking and antibody incubations were in PBS containing 0.05% Tween-20 and 3% BSA, at room temperature. DNA was stained with 0.1 μg/ml 4,6-diamidino-2-phenylindole (DAPI) and coverslips were mounted using Vectashield. Primary antibodies were: mouse anti-Aurora-A (0.2 μg/ml), goat anti-Aurora-A (0.1 μg/ml), rabbit anti-phospho-Aurora-A (Thr288; 1:100), mouse anti-mCherry (2.2 μg/ml), rabbit anti-GFP (1:500), mouse anti-NuMA (2 μg/ml), rabbit anti-NuMA (1:100), rabbit anti-pericentrin (2 μg/ml), mouse anti-α-tubulin B512 (2 μg/ml), mouse anti-α-tubulin DM1A (1:300), chicken anti-α-tubulin (1:100), mouse anti-γ-tubulin (21.8 μg/ml), mouse anti-TPX2 (4 μg/ml), rabbit anti-TPX2 (1:1500), rat anti-EB1 (1:100), rabbit anti-CEP-135 (1:5000), rabbit anti-Eg5 (1:1000).

For measurement of astral MT lengths, hTERT-RPE-1 cells were fixed for 10 min in −20°C methanol, followed by blocking at room temperature for 1 h using 5% (w/v) BSA dissolved in PBS. Cells were incubated with primary antibodies diluted in 5% BSA at 37°C for 1 h in a humidified chamber. After washing the cells with PBS for 30 min, the same procedure was repeated with dilutions of appropriate secondary antibodies. DNA was stained using 0.5 μg/ml DAPI for 1 min, and after washing, the coverslips were mounted in Mowiol mounting media.

in situ Proximity Ligation Assays (*is*PLA)

*is*PLA was performed on cells grown on coverslips and fixed with formaldehyde (see previous section) using the Duolink PLA kit according to manufacturer's instructions. The amplification time was 150 min for all tested interactions. Primary antibodies were used

Please cite this article in press as: Polverino et al., The Aurora-A/TPX2 Axis Directs Spindle Orientation in Adherent Human Cells by Regulating NuMA and Microtubule Stability, Current Biology (2020), https://doi.org/10.1016/j.cub.2020.10.096

(final concentrations as in IF) in pairs to detect the interactions, as follows: (i) mouse anti-Aurora-A/rabbit anti-TPX2 (Novus Biologicals); (ii) mouse anti-Aurora-A/rabbit anti-NuMA; (iii) mouse anti-NuMA/rabbit anti-TPX2 (Novus Biologicals); (iv) mouse anti-NuMA/rabbit anti-GFP. When indicated, a single primary antibody was used as control (CTR-) of the specificity of the interaction. In the same reactions, IF stainings were performed using indicated antibodies. DNA was stained with DAPI as above.

Microscopy analyses on fixed samples

Samples were analyzed using a Nikon Eclipse 90i microscope equipped with 100x (oil immersion; N.A. 1.3) objective and a Qicam Fast 1394 CCD camera (QImaging) or with an inverted microscope (Eclipse Ti, Nikon) using a 60x (oil immersion, N.A. 1.4) objective and the Clara camera (ANDOR technology). Images were acquired using Nis-Elements AR 3.2 (Nikon) or Nis-Elements H.C. 5.11 using the JOBS module for automated acquisitions; elaboration and processing was performed using Nis-Elements HC 5.02 (Nikon) and Adobe Photoshop CS 8.0.

For astral MTs length analysis, images were taken using the 3i Marianas spinning disk confocal system (Intelligent Imaging Innovations Inc.) equipped with Axio Observer Z1 microscope (Zeiss), Plan-Apochromat 60x 1.4 N.A. Oil Objective, M27 with DIC III Prism (Zeiss), Orca Flash 4.0 sCMOS Camera (Hamamatsu Photonics) and controlled by Slidebook Software 6.0 (Intelligent Imaging Innovations Inc.). Serial Z stacks of 0.3 μm thickness were acquired, taking care to cover the entire cell volume.

Spindle orientation analysis

For spindle orientation analyses, images of metaphase cells were acquired with 100x or 60x objectives along the z axis every 0.4 μm for a total range varying from cell to cell, so to include both spindle poles, detected by pericentrin or γ-tubulin staining. The angle between the spindle axis and the cell growth surface was calculated as previously described[17], using the "arctan(z/xy)" formula with "xy" being the distance between centrosomes in xy in the maximum intensity projection, and "z" being the distance between centrosomes along the z axis. Single measures used in the formula (pole-to-pole distances in z and xy dimensions) are reported in Figure S4, for the main conditions.

Quantitative analysis of fluorescent signals

For quantification of fluorescence intensity signals, images of mitotic cells were acquired using 60x or 100x objectives, along the z axis every 0.4-0.6 μm for a range of 8-10 μm. Signals were measured using Nis Elements H.C. 5.02 (nd2 file format) as follows: sum intensity values in the whole cell (TPX2/NuMA, GFP/NuMA or Aurora-A/TPX2 *is*PLAs; Aurora-A IF signal), at the mitotic spindle (Aurora-A/NuMA *is*PLA; Eg5, TPX2, α-tubulin; NuMA as indicated) or at single spindle poles (p-Thr-288 Aurora-A; NuMA as indicated). Images were corrected for external background, unless differently indicated in Figure legends.

For measuring astral MT lengths, the protocol was adapted from [44] and image quantification was performed on unmodified 16-bit z series images using Imaris 7.6.4 32-bit software (Bitplane). All images were opened and analyzed in the 'Surpass' mode of the software. The spindle width was manually determined using the tubulin channel, and the 3D position of the spindle poles was determined by using the 'Measurement' function on the CEP-135 signal. This was used to determine the internal spindle angle, defined as $arctan^{-1}$(spindle width / spindle length; see also [45]). The 'Spots' function was used to determine spherical coordinates of all EB1 comets using the spot diameter thresholded at 0.5 μm with application of occasional manual filtering to remove spots not also visibly associated with tubulin. These coordinates were extracted using the 'Statistics' function on Imaris and used to calculate the distance between all comets to the two poles using custom code written on MATLAB. The shorter of the two distances was used as a proxy for MT length. The angle between the line formed by a comet and its closest pole and the line formed by the two spindle poles was calculated using the cosine law. An EB1 comet was scored as belonging to an astral MT when this angle was greater than the internal spindle angle. The number of astral MTs per cell and the average astral MT length per cell were then calculated. For detection of number of MTs contacting the cortex, the protocol developed by [46] was utilized. Briefly, the cytoplasmic intensity of CEP-135 was used to determine the outline of cells in maximum intensity projection images of 16-bit raw images. Tubulin fluorescent intensities across a line drawn toward the inside of the cell boundary were extracted using the Plot Profile plugin from ImageJ. An average background value obtained from 3 random points lacking tubulin along the same line was subtracted from absolute intensities at all points. A threshold value (determined from visual inspection of correctly annotated MTs in 4 cells per experiment) was applied to background-corrected tubulin intensities. The number of MTs thus obtained was divided by the length of the cortex.

Immunoprecipitation (IP) assays and western blotting

Cells were lysed in culture dishes (total cell extracts) or harvested by shaking-off of non-adherent cells from cultures incubated with the Eg5 inhibitor Monastrol (100 μM, 16 h; mitotic extracts), and then lysed with RIPA buffer, supplemented with protease and phosphatase inhibitors. 30 μg of extract per lane were loaded on SDS-PAGE gels and transferred onto a nitrocellulose membrane using a semi-dry system.

In IP experiments, after 32 h from transfection, cells were treated with 100 μM Monastrol for 16 h, then lysed and processed for IP of GFP-tagged proteins using the GFP-Trap kit, according to manufacturer's instructions. Beads were incubated with total cell lysate (2 mg) for 3 h at 4°C, then washed and re-suspended in SDS-sample buffer and boiled to dissociate immune-complexes. About one-third of the immunoprecipitates and 50 μg of the whole lysates were loaded onto SDS-PAGE gels and transferred onto a nitrocellulose membrane using a wet system.

Please cite this article in press as: Polverino et al., The Aurora-A/TPX2 Axis Directs Spindle Orientation in Adherent Human Cells by Regulating NuMA and Microtubule Stability, Current Biology (2020), https://doi.org/10.1016/j.cub.2020.10.096

Membranes were blocked in TBS containing 5% low fat milk (or 5% BSA for anti-phospho-Aurora-A) and 0.1% Tween-20 and incubated at room temperature for 1 hour with primary antibodies (overnight incubation for anti-phospho-Aurora-A and Abcam anti-TPX2) followed by 30 minutes with secondary antibodies. HRP-conjugated secondary antibodies were revealed using the ECL western blotting detection reagent (Biorad). Primary antibodies used were: goat anti-actin (0.2 μg/ml), mouse anti-Aurora-A (0.4 μg/ml), rabbit anti-phospho-Aurora-A (Thr288; 1:500), mouse anti-GAPDH (1:1000), mouse anti-GFP (0.4 μg/ml), rabbit anti-NuMA (1:1000), mouse anti-TPX2 (4 μg/ml), rabbit anti-TPX2 (1:500; Novus Biologicals), rabbit anti-TPX2 (0.025 μg/ml;[14]).

QUANTIFICATION AND STATISTICAL ANALYSIS

Data from at least 3 experiments (sample size indicated in figure legends) were statistically analyzed using the InStat3 Graphpad 7 by: (i) unpaired Student's t tests and ordinary One-way Anova multiple comparison tests for measurements of continuous variables; when samples were not normally distributed Mann-Whitney and Kruskal-Wallis, respectively, were used instead; (ii) chi-square (and Fisher's exact) tests, in the contingency tables analyses for measurements of categorical variables; (iii) Pearson (normally distributed samples) or Spearman (non-normally distributed samples) correlation for single cell correlation analyses. The criterion for statistical significance (*) was set at $p < 0.01$.